Computers and Structures 245 (2021) 106433

Contents lists available at ScienceDirect

Computers and Structures

journal homepage: www.elsevier.com/locate/compstruc

New insights into the β_1/β_2-Bathe time integration scheme when L-stable

Mohammad Mahdi Malakiyeh [a], Saeed Shojaee [a], Saleh Hamzehei-Javaran [a], Klaus-Jürgen Bathe [b,*]

[a] Department of Civil Engineering, Shahid Bahonar University of Kerman, Kerman, Iran
[b] Massachusetts Institute of Technology Cambridge, MA 02139, United States

ARTICLE INFO

Article history:
Received 24 September 2020
Accepted 28 October 2020
Available online 23 December 2020

Keywords:
Transient dynamics
β_1/β_2-Bathe method
ρ_∞-Bathe method
L-stability
Numerical damping
Accuracy of solution

ABSTRACT

In this paper we focus on the L-stable β_1/β_2-Bathe time integration method to obtain new insights for transient and wave propagation solutions. The method is a specific case of the ρ_∞- Bathe scheme but deserves special attention because it can be used directly as a first-order and second-order scheme effective in certain analyses. We show how the parameters β_1 and β_2 can be used to introduce appropriate numerical damping and illustrate the theoretical findings through the solution of some wave propagation problems.

1. Introduction

Direct time integration methods are widely used to solve time dependent finite element equations. These methods are divided into two main categories: implicit and explicit techniques. Implicit methods can be conditionally and unconditionally stable, whereas the explicit methods are only conditionally stable [1]. Of particular interest are the unconditionally stable implicit methods because when using such a scheme the time step size is only governed by accuracy considerations. The disadvantage is that the computations per time step are significantly larger than when using an explicit scheme. Both types of methods are employed for solving problems of wave propagation and structural dynamics. While explicit schemes are mostly employed in the solution of wave propagations, the use of an effective unconditionally stable implicit scheme is very attractive because of the stability of the scheme [1]. The key for use of an implicit time integration method is that an accurate solution of the physical problem needs to be obtained with a coarser mesh and less time steps (than when using explicit time integration) with a resulting smaller total solution cost.

Numerical damping is an important feature of direct time integration methods (implicit or explicit) and its importance has been much researched, see for example Refs. [1–24]. The use of numerical damping can prevent the participation of spurious high frequencies (only present due to the mesh used) in a finite element system and many methods can be employed with numerical damping. The superiority of one method over another is established when a method can be used with a larger time step and less "total computational effort" for a given solution accuracy of physical problems.

The stability of a method is measured based on its spectral radius $\rho(\mathbf{A})$, a method can be A-stable or L-stable. A method is A-stable if $\rho(\mathbf{A}) \leqslant 1$ whereas a method is L-stable if it is A-stable and $\rho(\mathbf{A}) \to 0$ as $(\Delta t/T) \to \infty$, where, considering a generic single degree of freedom system, T is its natural period of vibration, Δt is the time step used. When a large finite element system is considered T is the smallest period in the system [1,5,6].

The generality of a method is reflected when the magnitude of the spectral radius for a given $\Delta t/T$, including when $(\Delta t/T) \to \infty$, can be adjusted. However, of much interest for the solution of many physical problems are L-stable techniques, and in such a scheme we desire an "effective amplitude decay together with small period elongation errors".

The numerical amplitude decay is governed by the value of the spectral radius. As long as $\rho(\mathbf{A}) = 1$, the method does not display numerical damping, like for the Trapezoidal Rule for any $\Delta t/T$ and for other methods as long as $\Delta t/T$ is small. But when $\rho(\mathbf{A}) < 1$ numerical damping is present, the amount is given by the magnitude of $\rho(\mathbf{A})$, and ideally the decrease of $\rho(\mathbf{A})$ from 1 is rapid at a large value of $\Delta t/T$. We shall call the value of $\Delta t/T$ at which the "fall" of $\rho(\mathbf{A})$ from $\rho(\mathbf{A}) = 1$ occurs, the "fall-value" (see Fig. 1a for an example).

Among the well-known methods that are L-stable, we have the Houbolt method [1,2], the Newmark method when used with

* Corresponding author.
E-mail address: kjb@mit.edu (K.J. Bathe).

https://doi.org/10.1016/j.compstruc.2020.106433
0045-7949/

appropriate parameters [1,3], the Wilson method [1,4,5], the HHT method [7], the 3-parameter [8] and the Bathe methods [1,9,10] (see Section 2). The Houbolt, Newmark, Wilson, HHT and 3-parameter schemes are one-step methods, while the Bathe methods split the time step and consider an additional solution for the sub-step. Hence, the Bathe methods may be considered two step schemes, although the calculations "internal" to the full step are better regarded as part of the calculations per step. A particular attractive feature of the Bathe methods is that the spectral radius can, be changed quite effectively.

The "standard Bathe method" [9,10] is *L*-stable and second order accurate for all values of the time step splitting ratio, called γ. By changing γ, we can change the fall-value and obtain different solution characteristics of the scheme. Initially, focus was on the value $\gamma = 0.5$ for simplicity and because overall good solution accuracy was obtained [10].

In addition, we introduced the β_1/β_2-Bathe method [21], in which the first sub-step is as in the standard Bathe scheme and the second sub-step uses a weighted assumption on velocities and accelerations for the complete step. This method uses three control parameters including the time step splitting ratio. We assumed in Ref. [21] that the time step splitting ratio is constant, $\gamma = 0.5$.

As a generalization of the above schemes, the ρ_∞-Bathe method was presented [22,23], which we discuss briefly below. The ρ_∞-Bathe method contains as special cases the standard Bathe method and the β_1/β_2-Bathe scheme. However, normally the ρ_∞-Bathe scheme is used as a second-order method whereas the β_1/β_2–Bathe method can be of first order. In Ref. [24], both, the β_1/β_2-Bathe and ρ_∞-Bathe methods were used in solving wave propagation problems achieving good results but demonstrating also that the use of a first order method may be valuable for wave propagation problems. This observation spurred our further research into the β_1/β_2-Bathe scheme, in particular also considering the cases when the splitting ratio $\gamma \neq 0.5$.

In this paper, the β_1/β_2-Bathe time integration method is further studied when the value of γ is changed, thus having three control parameters. However, for practical use, we reduce these parameters to two and even one, and show how to apply desired numerical damping in the *L*-stable state of the method. In addition, we compare the β_1/β_2-Bathe scheme with the standard Bathe scheme using different values of γ (which is the ρ_∞-Bathe method in the *L*-stable state) by spectral radii, amplitude decays and period elongations, and provide some recommendations for use of the schemes. We also give illustrative example solutions to show the performance of the methods.

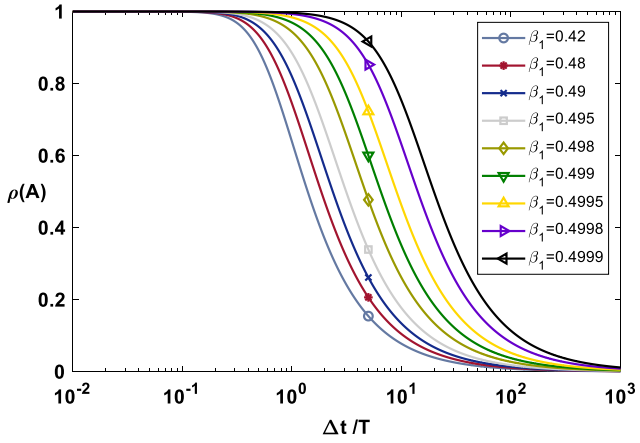

Fig. 1a. Spectral radius of second order accurate case for various β_1. The "fall-value" for the case $\beta_1 = 0.4999$ is about 1.0.

We should point out that throughout the paper we assume that traditional spatial finite element discretizations are used [1]. However, the findings presented here are also of value when using "overlapping finite elements" [25,26].

2. The Bathe time integration schemes

The Bathe time integration schemes are based on the original method proposed in refs. [9,10]. In this approach the time step is divided into two sub-steps, $\gamma\Delta t$ and $(1-\gamma)\Delta t$. For the first sub-step the Trapezoidal Rule is used and for the second sub-step the three-point Euler backward method is employed. Here the time step splitting ratio γ is a variable although it was found that using the "simple" value γ = 0.5 was quite effective, in linear and nonlinear analyses [10,27].

The use of more than two sub-steps per full time step was also briefly explored in ref. [9], but then not focused on.

The basic idea of combining the trapezoidal rule and Euler backward method in two sub-steps for one full time step is simple: to obtain a method which is unconditionally stable with some, but not too severe, amplitude decay. Of course, the Trapezoidal Rule and Euler method are unconditionally stable, the Trapezoidal Rule does not give amplitude decay whereas the Euler method shows too much amplitude decay. Hence the prospect of using the two techniques in one scheme was promising. However, researchers in finite element analyses had prior focused only on single-step methods, see for example Refs. [7,8].

This scheme was termed the "standard Bathe method", it is *L*-stable for all values of the time step splitting ratio, called γ. By changing γ , we can change the fall-value. The method is second order accurate for all values of γ and was very successfully used to solve problems in industry that were difficult to solve accurately using other schemes [28,29]

New insights into the standard Bathe method were presented in refs. [11,17,22] where the behavior of the scheme was shown for varying values of γ, resulting into different spectral radii. In these studies also values of $\gamma > 1$ were considered, with the studies showing that numerical damping could be introduced with appropriate values of γ.

Recently, we introduced the β_1/β_2-Bathe method [21], in which the Trapezoidal Rule is employed in the first sub-step and the same weighted assumption for velocities (to calculate the new displacements) and accelerations (to calculate the new velocities) twice using the three time points for the second sub-step. This method uses in principle three control parameters: two are the β_1/β_2 parameters used for the second sub-step, and the third is the time step splitting ratio. We assumed in Ref. [21] the time step splitting ratio to be constant, $\gamma = 0.5$, and the method then contains the standard Bathe method (using $\gamma = 0.5$). We considered two cases of changing β_1 and β_2. The first case ($\beta_2 = 1 - \beta_1$) is *A*-stable and second order accurate, and the second case ($\beta_2 = 2\beta_1$) is *L*-stable, and first or second order accurate depending on the values chosen. In the first case, we can adjust the amount of numerical damping, and in the second case, we can change the fall-value of the spectral radius.

As a generalization of the above schemes, the ρ_∞-Bathe method was presented [22]. In the first sub-step, the Trapezoidal Rule is used for the equilibrium at time $t + \gamma\Delta t$,

$$\mathbf{M}\,{}^{t+\gamma\Delta t}\ddot{\mathbf{U}} + \mathbf{C}\,{}^{t+\gamma\Delta t}\dot{\mathbf{U}} + \mathbf{K}\,{}^{t+\gamma\Delta t}\mathbf{U} = {}^{t+\gamma\Delta t}\mathbf{R} \tag{1}$$

$${}^{t+\gamma\Delta t}\mathbf{U} = {}^{t}\mathbf{U} + \frac{\gamma\Delta t}{2}({}^{t}\dot{\mathbf{U}} + {}^{t+\gamma\Delta t}\dot{\mathbf{U}}) \tag{2}$$

$${}^{t+\gamma\Delta t}\dot{\mathbf{U}} = {}^{t}\dot{\mathbf{U}} + \frac{\gamma\Delta t}{2}({}^{t}\ddot{\mathbf{U}} + {}^{t+\gamma\Delta t}\ddot{\mathbf{U}}) \tag{3}$$

and in the second sub-step, the following relations for the equilibrium at time $t+\Delta t$ are employed

$$\mathbf{M}\,{}^{t+\Delta t}\ddot{\mathbf{U}} + \mathbf{C}\,{}^{t+\Delta t}\dot{\mathbf{U}} + \mathbf{K}\,{}^{t+\Delta t}\mathbf{U} = {}^{t+\Delta t}\mathbf{R} \tag{4}$$

$${}^{t+\Delta t}\mathbf{U} = {}^{t}\mathbf{U} + \Delta t\,(q_0\,{}^{t}\dot{\mathbf{U}} + q_1^{t+\gamma\Delta t}\dot{\mathbf{U}} + q_2\,{}^{t+\Delta t}\dot{\mathbf{U}}) \tag{5}$$

$${}^{t+\Delta t}\dot{\mathbf{U}} = {}^{t}\dot{\mathbf{U}} + \Delta t\,(s_0{}^{t}\ddot{\mathbf{U}} + s_1\,{}^{t+\gamma\Delta t}\ddot{\mathbf{U}} + s_2\,{}^{t+\Delta t}\ddot{\mathbf{U}}) \tag{6}$$

where $s_0, s_1, s_2, q_0, q_1, q_2$ are parameters. In principle, these parameters can be determined in various ways to achieve unconditional stability and good accuracy. The accuracy is measured by the amplitude decay and period elongation.

To obtain the final equations used in the ρ_∞-Bathe method, we use Eqs. (5) and (6), impose that second order accuracy be obtained and thus establish all constants. With this approach all parameters are set, except the time step splitting ratio γ and the spectral radius ρ_∞. These determine the characteristics of the time integration scheme. While γ and ρ_∞ are independent parameters, it is effective to use the optimal value of γ for a given ρ_∞

For $\rho_\infty \in [0,1]$, the scheme provides identical effective stiffness matrices for the two sub-steps, a local maximum of amplitude decay within the range of $\gamma \in (0,\ 1)$ and the global minimum of the period elongation with the following γ:

$$\gamma_0 = \frac{2-\sqrt{2+2\rho_\infty}}{1-\rho_\infty};\gamma_0 = 0.5 \quad \text{if } \rho_\infty = 1 \tag{7}$$

With the relation in Eq. (7), the method is a "one-parameter scheme". In the method, we can adjust the fall-value of the spectral radius and the value of ρ_∞. The method is *A*-stable for all values of γ, and *L*-stable for $\rho_\infty = 0$ and all values of γ. The method is the standard Bathe scheme when using ρ_∞ = 0 and with specific values of the constants $s_0, s_1, s_2, q_0, q_1, q_2$, the ρ_∞-Bathe method also reduces to the β_1/β_2-Bathe method [23].

In the initial study [22], the method was introduced as a second order accurate method for $\rho_\infty \in [0,\ 1]$, then in Ref. [23], a first order accurate scheme of the ρ_∞-Bathe was introduced and the use of $\rho_\infty \in [-1,\ 0]$ was investigated. To obtain further insight, the ρ_∞-Bathe method was compared with the Newmark method [23], where it was shown that the commonly used time integration scheme of the Newmark method is also contained in the ρ_∞-Bathe procedure.

3. The β_1/β_2-Bathe time integration method

In this section we first present the basic equations of the β_1/β_2-Bathe scheme including the splitting ratio γ as a parameter and then give the stability analysis.

3.1. The basic equations

In the β_1/β_2-Bathe time integration method, we use the two sub-steps of size $\gamma\Delta t$ and $(1-\gamma)\Delta t$ [21]. For the first sub-step we use

$${}^{t+\gamma\Delta t}\dot{\mathbf{U}} = -\frac{2}{(\gamma\Delta t)}\,{}^{t}\mathbf{U} - {}^{t}\dot{\mathbf{U}} + \frac{2}{(\gamma\Delta t)}\,{}^{t+\gamma\Delta t}\mathbf{U} \tag{8}$$

$${}^{t+\gamma\Delta t}\ddot{\mathbf{U}} = -\frac{4}{(\gamma\Delta t)^2}\,{}^{t}\mathbf{U} - \frac{4}{(\gamma\Delta t)}\,{}^{t}\dot{\mathbf{U}} - {}^{t}\ddot{\mathbf{U}} + \frac{4}{(\gamma\Delta t)^2}\,{}^{t+\gamma\Delta t}\mathbf{U} \tag{9}$$

and

$$\mathbf{M}\,{}^{t+\gamma\Delta t}\ddot{\mathbf{U}} + \mathbf{C}\,{}^{t+\gamma\Delta t}\dot{\mathbf{U}} + \mathbf{K}\,{}^{t+\gamma\Delta t}\mathbf{U} = {}^{t+\gamma\Delta t}\mathbf{R} \tag{10}$$

Substituting from Eqs. (8) and (9) into Eq. (10), we obtain

$$\hat{\mathbf{K}}_1\,{}^{t+\gamma\Delta t}\mathbf{U} = {}^{t+\gamma\Delta t}\hat{\mathbf{R}}_1 \tag{11}$$

where

$$\hat{\mathbf{K}}_1 = \frac{4}{(\gamma\Delta t)^2}\mathbf{M} + \frac{2}{(\gamma\Delta t)}\mathbf{C} + \mathbf{K} \tag{12}$$

$${}^{t+\gamma\Delta t}\hat{\mathbf{R}}_1 = {}^{t+\gamma\Delta t}\mathbf{R} + \mathbf{M}\left[\frac{4}{(\gamma\Delta t)^2}\,{}^{t}\mathbf{U} + \frac{4}{\gamma\Delta t}\,{}^{t}\dot{\mathbf{U}} + {}^{t}\ddot{\mathbf{U}}\right] + \mathbf{C}\left[\frac{2}{\gamma\Delta t}\,{}^{t}\mathbf{U} + {}^{t}\dot{\mathbf{U}}\right] \tag{13}$$

and we use our usual notation for displacements, velocities, acceleration, stiffness, mass and damping matrices, and time stepping [1].

For the second sub-step, the governing equations are

$$\begin{aligned}{}^{t+\Delta t}\dot{\mathbf{U}} = &-\frac{1}{\beta_2(1-\gamma)\Delta t}\,{}^{t}\mathbf{U} - \frac{\gamma(1-\beta_1)}{\beta_2(1-\gamma)}\,{}^{t}\dot{\mathbf{U}} \\ &- \frac{\gamma\beta_1 + (1-\beta_2)(1-\gamma)}{\beta_2(1-\gamma)}\,{}^{t+\gamma\Delta t}\dot{\mathbf{U}} + \frac{1}{\beta_2(1-\gamma)\Delta t}\,{}^{t+\Delta t}\mathbf{U}\end{aligned} \tag{14}$$

$$\begin{aligned}{}^{t+\Delta t}\ddot{\mathbf{U}} = &\frac{1}{(\beta_2(1-\gamma)\Delta t)^2}\,{}^{t}\mathbf{U} - \frac{\gamma(1-\beta_1)+\beta_2(1-\gamma)}{(\beta_2(1-\gamma))^2\Delta t}\,{}^{t}\dot{\mathbf{U}} - \frac{\gamma(1-\beta_1)}{\beta_2(1-\gamma)}\,{}^{t}\ddot{\mathbf{U}} \\ &- \frac{\gamma\beta_1 + (1-\beta_2)(1-\gamma)}{(\beta_2(1-\gamma))^2\Delta t}\,{}^{t+\gamma\Delta t}\dot{\mathbf{U}} - \frac{\gamma\beta_1 + (1-\beta_2)(1-\gamma)}{\beta_2(1-\gamma)}\,{}^{t+\gamma\Delta t}\ddot{\mathbf{U}} \\ &+ \frac{1}{(\beta_2(1-\gamma)\Delta t)^2}\,{}^{t+\Delta t}\mathbf{U}\end{aligned} \tag{15}$$

$$\mathbf{M}\,{}^{t+\Delta t}\ddot{\mathbf{U}} + \mathbf{C}\,{}^{t+\Delta t}\dot{\mathbf{U}} + \mathbf{K}\,{}^{t+\Delta t}\mathbf{U} = {}^{t+\Delta t}\mathbf{R} \tag{16}$$

Substituting from Eqs. (14) and (15) into Eq. (16) we obtain

$$\hat{\mathbf{K}}_2\,{}^{t+\Delta t}\mathbf{U} = {}^{t+\Delta t}\hat{\mathbf{R}}_2 \tag{17}$$

where

$$\hat{\mathbf{K}}_2 = \frac{1}{(\beta_2(1-\gamma)\Delta t)^2}\mathbf{M} + \frac{1}{\beta_2(1-\gamma)\Delta t}\mathbf{C} + \mathbf{K} \tag{18}$$

$$\begin{aligned}{}^{t+\Delta t}\hat{\mathbf{R}}_2 = {}^{t+\Delta t}\mathbf{R} + \mathbf{M}&\left[\frac{1}{(\beta_2(1-\gamma)\Delta t)^2}\,{}^{t}\mathbf{U} + \frac{\gamma(1-\beta_1)+\beta_2(1-\gamma)}{(\beta_2(1-\gamma))^2\Delta t}\,{}^{t}\dot{\mathbf{U}}\right. \\ &+ \frac{\gamma\beta_1 + (1-\beta_2)(1-\gamma)}{(\beta_2(1-\gamma))^2\Delta t}\,{}^{t+\gamma\Delta t}\dot{\mathbf{U}} + \frac{\gamma(1-\beta_1)}{\beta_2(1-\gamma)}\,{}^{t}\ddot{\mathbf{U}} \\ &\left.+ \frac{\gamma\beta_1 + (1-\beta_2)(1-\gamma)}{\beta_2(1-\gamma)}\,{}^{t+\gamma\Delta t}\ddot{\mathbf{U}}\right] + \mathbf{C}\left[\frac{1}{\beta_2(1-\gamma)\Delta t}\,{}^{t}\mathbf{U}\right. \\ &\left.+ \frac{\gamma(1-\beta_1)}{\beta_2(1-\gamma)}\,{}^{t}\dot{\mathbf{U}} + \frac{\gamma\beta_1 + (1-\beta_2)(1-\gamma)}{\beta_2(1-\gamma)}\,{}^{t+\gamma\Delta t}\dot{\mathbf{U}}\right]\end{aligned} \tag{19}$$

3.2. Stability analysis

To study the stability and accuracy of the β_1/β_2-Bathe method, we use the procedure given, for example, in refs. [1,5,6] and establish the following recursive formula

$$\begin{bmatrix}{}^{t+\Delta t}u\\ {}^{t+\Delta t}\dot{u}\\ {}^{t+\Delta t}\ddot{u}\end{bmatrix} = \mathbf{A}\begin{bmatrix}{}^{t}u\\ {}^{t}\dot{u}\\ {}^{t}\ddot{u}\end{bmatrix} + \mathbf{L}_a\,{}^{t+\gamma\Delta t}r + \mathbf{L}\,{}^{t+\Delta t}r \tag{20}$$

where **A, L**$_a$ and **L** are the amplification matrix and load operators. The amplification matrix contains as variables $\Delta t/T$, ξ, β_1, β_2, γ, where ξ is the damping ratio [1].

For the analysis of the method, the spectral radius of the matrix **A** defined as

$$\rho(\mathbf{A}) = \max_i |\lambda_i(\mathbf{A})| \tag{21}$$

is used where λ_i are the eigenvalues of the matrix. A method is L-stable if $\rho(\mathbf{A}) \leqslant 1$ and $\rho(\mathbf{A}) \to 0$ as $(\Delta t/T) \to \infty$. The accuracy of a direct time integration method is measured by establishing the amplitude decay and period elongation [1].

3.3. L-Stability

In this paper we only focus on the case of L-stability of the methods.

Assuming no physical damping (that is, the damping ratio $\xi = 0$)$(\Delta t/T) \to \infty$, the three eigenvalues (λ_i) of $\mathbf{A}$ are

$$\begin{aligned} &\lim_{\frac{\Delta t}{T}\to\infty} \lambda_{1,2} = \frac{-(2\beta_1\gamma - 2\gamma - \beta_2 + \beta_2\gamma + 1)}{\beta_2(\gamma - 1)} \quad \to \quad \lambda_{1,2}^{\infty} = \frac{-(2\beta_1\gamma - 2\gamma - \beta_2 + \beta_2\gamma + 1)}{\beta_2(\gamma - 1)} \\ &\lim_{\frac{\Delta t}{T}\to\infty} \lambda_3 = 0 \quad \to \quad \lambda_3^{\infty} = 0 \end{aligned} \tag{22}$$

and for $(\Delta t/T) \to \infty$, we have

$$\rho_{\infty}(\mathbf{A}) = \max_i |\lambda_i^{\infty}(\mathbf{A})| = \left|\frac{-(2\beta_1\gamma - 2\gamma - \beta_2 + \beta_2\gamma + 1)}{\beta_2(\gamma - 1)}\right| \tag{23}$$

Hence for L-stability we need to have

$$2\beta_1\gamma - 2\gamma - \beta_2 + \beta_2\gamma + 1 = 0 \tag{24}$$

which gives γ in terms of β_1 and β_2

$$\gamma = \frac{(\beta_2 - 1)}{(2\beta_1 - 2 + \beta_2)} \tag{25}$$

We want to use values of the splitting ratio satisfying $0 < \gamma < 1$ and obtain with some arithmetic that for L-stability we should use (see also Section 3.4)

$$\begin{aligned} &\text{if} \quad 0 < \beta_1 < 0.5 \quad \to \quad \left[2(1-\beta_1) - 0.5(16\beta_1^2 - 24\beta_1 + 8)^{0.5}\right] \leqslant \beta_2 < 1 \\ &\text{if} \quad \beta_1 > 0.5 \quad \to \quad \beta_2 > 1 \end{aligned} \tag{26}$$

This method is a two-parameter scheme, not using $\beta_1 = 0.5$ because then $\gamma = 1$ (see Eq. (25)). Valuable properties are that considering a given value of β_1 in the range $0 < \beta_1 < 0.5$, the method can be second order or first order accurate (see Section 3.4), and the spectral radius fall-value decreases as we move from $\left[2(1-\beta_1) - 0.5(16\beta_1^2 - 24\beta_1 + 8)^{0.5}\right]$ to 1.

If we choose $\beta_1 > 0.5$, β_2 can be any value satisfying $\beta_2 > 1$, we have only first order accuracy, and the closer β_2 is to 1, the smaller the fall-value.

3.4. Order of accuracy

In the β_1/β_2-Bathe method, the local truncation errors of displacement, velocity and acceleration are

$$\begin{aligned} e_{\,t+\Delta t\mathbf{U}} &= -\left[(\beta_1 + \beta_2 - 1)\gamma^2 + (1 - 2\beta_2)\gamma + (\beta_1 - \tfrac{1}{2})\right]{}^t\ddot{\mathbf{U}}\Delta t^2 + o(\Delta t^3) \\ e_{\,t+\Delta t\dot{\mathbf{U}}} &= -\left[(\beta_1 + \beta_2 - 1)\gamma^2 + (1 - 2\beta_2)\gamma + (\beta_1 - \tfrac{1}{2})\right]{}^t\ddot{\mathbf{U}}\Delta t^2 + o(\Delta t^3) \\ e_{\,t+\Delta t\ddot{\mathbf{U}}} &= -\left[(\beta_1 + \beta_2 - 1)\gamma^2 + (1 - 2\beta_2)\gamma + (\beta_1 - \tfrac{1}{2})\right]\mathbf{M}^{-1} \\ &\quad \left[\mathbf{C}({}^t\ddot{\mathbf{U}}) + \mathbf{K}({}^t\ddot{\mathbf{U}})\right]\Delta t^2 + o(\Delta t^3) \end{aligned} \tag{27}$$

As seen in Eq. (27), the presence or absence of physical damping has no effect on the order of accuracy. We also see that second-order accuracy is obtained when satisfying

$$(\beta_1 + \beta_2 - 1)\gamma^2 + (1 - 2\beta_2)\gamma + (\beta_1 - \frac{1}{2}) = 0 \tag{28}$$

Using $\gamma = (\beta_2 - 1)/(2\beta_1 - 2 + \beta_2)$ (from Eq. (25)) in Eq. (28), we have

$$\begin{aligned} &(\beta_1 + \beta_2 - 1)\left(\frac{(\beta_2 - 1)}{(2\beta_1 - 2 + \beta_2)}\right)^2 + (1 - 2\beta_2)\left(\frac{(\beta_2 - 1)}{(2\beta_1 - 2 + \beta_2)}\right) \\ &\quad + (\beta_1 - \frac{1}{2}) = 0 \end{aligned} \tag{29}$$

To satisfy the stability requirements in Eq. (26), the following condition is obtained

$$\text{if} \quad 0 < \beta_1 < 0.5 \quad \to \quad \beta_2 = \frac{-(4\beta_1^2 - 6\beta_1 + 2) + \sqrt{2(2\beta_1 - 1)^3(\beta_1 - 1)}}{2(\beta_1 - 0.5)} \tag{30}$$

where if $0 < \beta_1 < 0.5$

$$\begin{aligned} &\frac{-(4\beta_1^2 - 6\beta_1 + 2) + \sqrt{2(2\beta_1 - 1)^3(\beta_1 - 1)}}{2(\beta_1 - \frac{1}{2})} \\ &\quad = \left[2(1-\beta_1) - 0.5(16\beta_1^2 - 24\beta_1 + 8)^{0.5}\right] \end{aligned} \tag{31}$$

Hence to have second order accuracy and L-stability with one parameter, the following equation can be used

$$\text{if} \quad 0 < \beta_1 < 0.5 \quad \to \quad \beta_2 = \left[2(1-\beta_1) - 0.5(16\beta_1^2 - 24\beta_1 + 8)^{0.5}\right] \tag{32}$$

Figs. 1a–1c shows the spectral radius, amplitude decay and period elongation for some values of β_1 with $0.41 < \beta_1 < 0.5$. These values may be effective for use in solutions. Fig. 1a also points out a fall-value, as an example.

Hence in summary, considering Eqs. (26) and (32), if $0 < \beta_1 < 0.5$, for $\left[2(1-\beta_1) - 0.5(16\beta_1^2 - 24\beta_1 + 8)^{0.5}\right] \leqslant \beta_2 < 1$ the method is L-stable and for $\beta_2 = \left[2(1-\beta_1) - 0.5(16\beta_1^2 - 24\beta_1 + 8)^{0.5}\right]$ the method is second order accurate. Then, as we use β_2 slightly greater than $\left[2(1-\beta_1) - 0.5(16\beta_1^2 - 24\beta_1 + 8)^{0.5}\right]$ and increase β_2 towards 1, the method is first order accurate and the fall-value of the spectral radius decreases. This characteristic is shown in Figs. 2a-2c, which also demonstrates that the amplitude decay increases which we shall use in solving wave propagation problems to try to obtain more accuracy in the solutions.

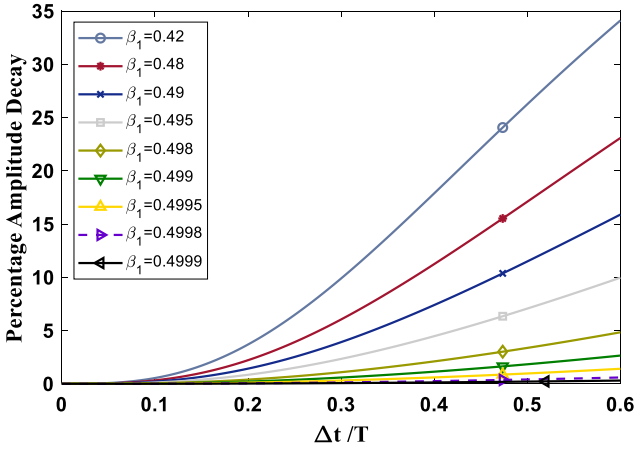

Fig. 1b. Percentage amplitude decay of second order accurate case for various β_1.

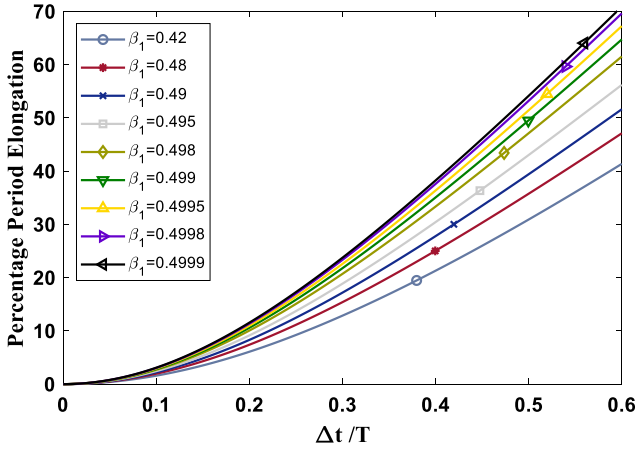

Fig. 1c. Percentage period elongation of second order accurate case for various β_1.

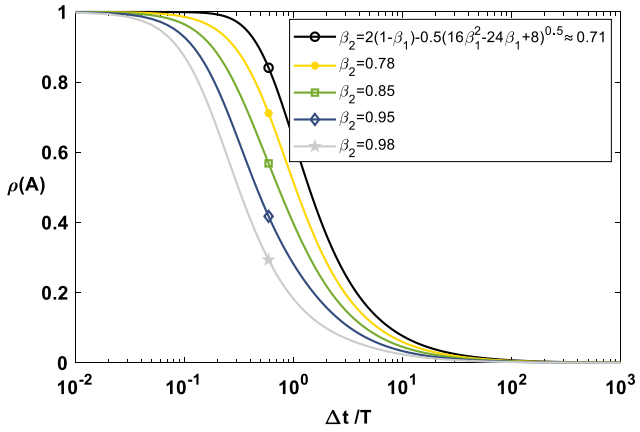

Fig. 2a. Spectral radius for $\beta_1 = 0.4$ and $[2(1-\beta_1) - 0.5(16\beta_1^2 - 24\beta_1 + 8)^{0.5}] \leqslant \beta_2 < 1$.

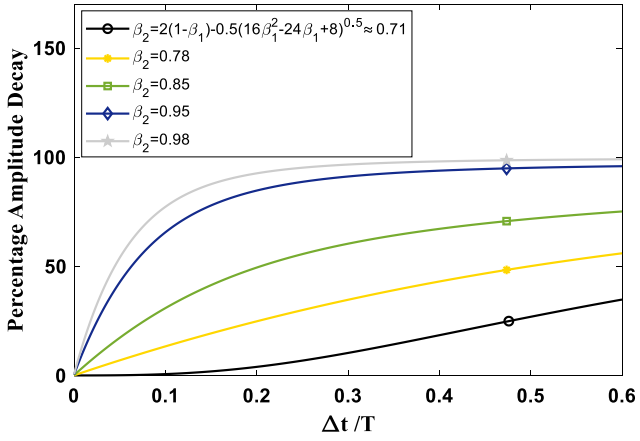

Fig. 2b. Percentage amplitude decay for $\beta_1 = 0.4$ and $[2(1-\beta_1) - 0.5(16\beta_1^2 - 24\beta_1 + 8)^{0.5}] \leqslant \beta_2 < 1$.

3.5. Using the splitting ratio $\gamma = 0.5$

The case $\beta_2 = 2\beta_1$ is important and has been introduced and analyzed earlier using $\gamma = 0.5$ [21]. The scheme is then L-stable using Eq. (25)

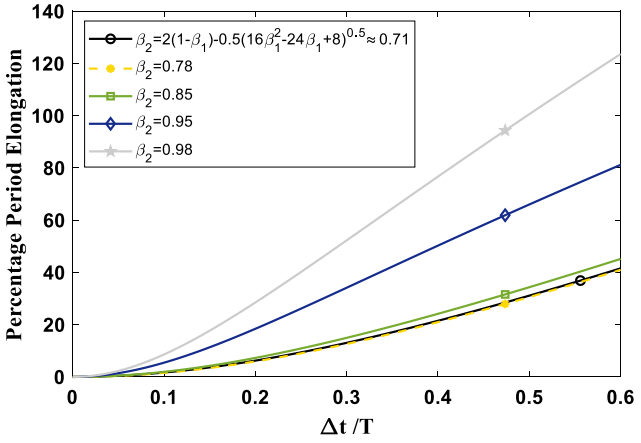

Fig. 2c. Percentage period elongation for $\beta_1 = 0.4$ and $[2(1-\beta_1) - 0.5(16\beta_1^2 - 24\beta_1 + 8)^{0.5}] \leqslant \beta_2 < 1$.

$$\gamma = 0.5 \quad \rightarrow \quad \frac{(\beta_2 - 1)}{(2\beta_1 - 2 + \beta_2)} = 0.5 \quad \rightarrow \quad \beta_2 = 2\beta_1 \tag{33}$$

and Eq. (26)

$$\begin{aligned} &\text{if} \quad \tfrac{1}{3} \leqslant \beta_1 < 0.5 \quad \rightarrow \quad \beta_2 = 2\beta_1 \\ &\text{if} \quad \beta_1 > 0.5 \quad \rightarrow \quad \beta_2 = 2\beta_1 \end{aligned} \tag{34}$$

The case $\beta_1 = 1/3$ is the standard Bathe scheme using $\gamma = 0.5$ and is second order accurate. For other values of β_1 the method is first order accurate. This scheme is also a one-parameter method which when increasing β_1 leads to more numerical damping.

3.6. Using the same effective stiffness matrix in both sub-steps

Using the same stiffness matrix in both sub-steps in linear analysis leads to a reduction of numerical operations. According to Eqs. (12) and (17), the same effective stiffness matrix is obtained if

$$2\beta_2(1-\gamma) - \gamma = 0 \tag{35}$$

With $\gamma = (\beta_2 - 1)/(2\beta_1 - 2 + \beta_2)$ we have

$$\frac{(4\beta_1\beta_2 - 3\beta_2 + 1)}{(2\beta_1 + \beta_2 - 2)} = 0 \tag{36}$$

To satisfy Eq. (36) and keep the L-stability (see Eq. (26)), the following conditions need to hold

$$\begin{aligned} &\text{if} \quad (0.75 - 0.25\sqrt{2}) \leqslant \beta_1 < 0.5 \quad \rightarrow \quad \beta_2 = \tfrac{1}{3-4\beta_1} \\ &\text{if} \quad 0.5 < \beta_1 < \tfrac{3}{4} \quad \rightarrow \quad \beta_2 = \tfrac{1}{3-4\beta_1} \end{aligned} \tag{37}$$

If we want to have L-stability, satisfy $0 < \gamma < 1$, second order accuracy and the same effective stiffness matrix in both sub-steps, Eqs. (32) and (37) have to be satisfied leading to the use of

$$\beta_1 = 0.75 - 0.25\sqrt{2} \quad \rightarrow \quad \beta_2 = \frac{1}{(3-4\beta_1)} \tag{38}$$

We summarize the various cases considered above in Table 1, where we should emphasize that in each case γ is given by Eq. (25). We mentioned earlier that in principle all constants for the β_1/β_2- Bathe scheme could be calculated for the ρ_∞-Bathe method using $\rho_\infty = 0$. The table shows that for some cases, the corresponding use of the ρ_∞-Bathe method is direct, because both constants β_1 and β_2 are simple. However, in other cases β_2 is shown by an expression and it is best to use β_2 directly as given in Table 1.

Table 1
Various cases of the β_1/β_2 – Bathe scheme when L-stable, $\gamma = (\beta_2 - 1)/(2\beta_1 - 2 + \beta_2)$.

Accuracy	β_1	β_2
second order accuracy, $0 < \gamma < 1$	$0 < \beta_1 < 0.5$	$\beta_2 = \left[2(1-\beta_1) - 0.5(16\beta_1^2 - 24\beta_1 + 8)^{0.5}\right]$
first order accuracy, $0 < \gamma < 1$	$0 < \beta_1 < 0.5$	$\left[2(1-\beta_1) - 0.5(16\beta_1^2 - 24\beta_1 + 8)^{0.5}\right] < \beta_2 < 1$
first order accuracy, $0 < \gamma < 1$	$\beta_1 > 0.5$	$\beta_2 > 1$
first order accuracy, $\gamma = 0.5$	$\frac{1}{3} < \beta_1 < 0.5$, $\beta_1 > 0.5$	$\beta_2 = 2\beta_1$
first order accuracy, $0 < \gamma < 1$, *same effective stiffness matrix*	$(0.75 - 0.25\sqrt{2}) < \beta_1 < 0.5$ $0.5 < \beta_1 < \frac{3}{4}$	$\beta_2 = \frac{1}{3-4\beta_1}$
second order accuracy, $0 < \gamma < 1$, *same effective stiffness matrix*	$\beta_1 = 0.75 - 0.25\sqrt{2}$	$\beta_2 = \frac{1}{3-4\beta_1}$

4. The β_1/β_2-Bathe scheme versus the standard Bathe scheme

As mentioned already, the ρ_∞-Bathe method using $\rho_\infty = 0$ is the standard Bathe method and is L-stable for all values of γ, in particular we can use $0 < \gamma < 2$, $\gamma \neq 1$.

Considering the values $1.17 < \gamma < 2$ we find that the fall-value of the spectral radius of the standard Bathe method decreases from the value for $\gamma = 0.5$ which may be useful in the solution of wave propagation problems. Figs. 3a–3c gives the spectral radii, amplitude decays and period elongations of the standard Bathe method for $1.17 < \gamma < 2$ in comparison to the values with $\gamma = 0.5$. As seen in Figs. 3a–3c, the period elongation increases greatly as more numerical damping is used. Figs. 4a–4c shows the same information for the β_1/β_2- Bathe method using $\beta_1 = 0.43$ and $\left[2(1-\beta_1) - 0.5(16\beta_1^2 - 24\beta_1 + 8)^{0.5}\right] \leqslant \beta_2 < 1$ (with Eqs. (25) and (26)) and gives a comparison with the standard Bathe method. We see that the β_1/β_2- Bathe scheme period elongation error is much less than when using the standard scheme. Hence we can expect that the β_1/β_2- Bathe scheme will perform better, give more accuracy, in some solutions. On the other hand, when the desired amplitude decay is huge, any errors in the period may not have significant consequences.

5. Recommendations for using the Bathe integration schemes: a recipe

With the choice of parameters available in the Bathe schemes, the question might be how to best tackle in practice the solution of a structural vibration or wave propagation problem using the methods. Our aim is here to give some guidelines, in effect suggest "a recipe" for use.

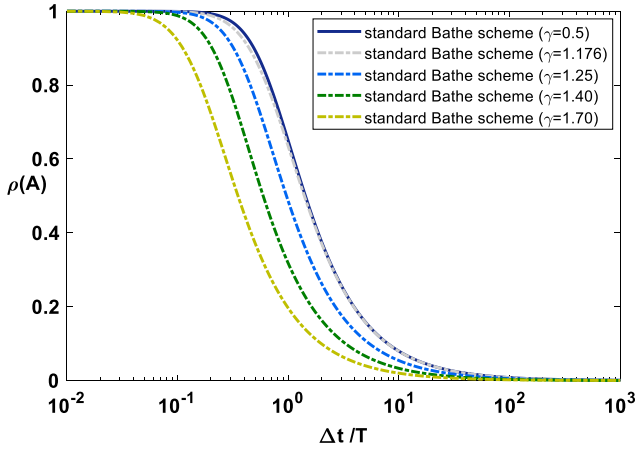

Fig. 3a. Spectral radius of standard Bathe scheme for various γ.

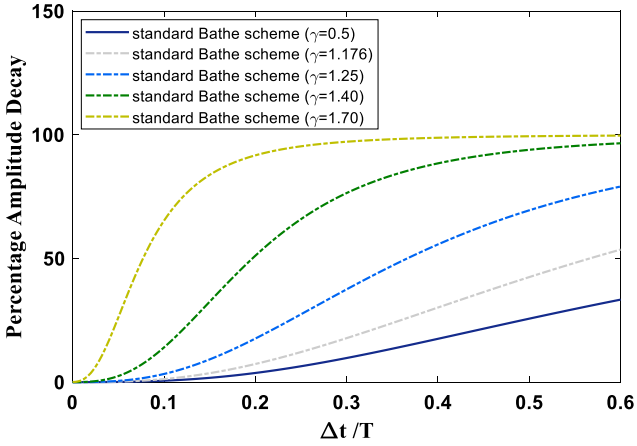

Fig. 3b. Percentage amplitude decay of standard Bathe scheme for various γ.

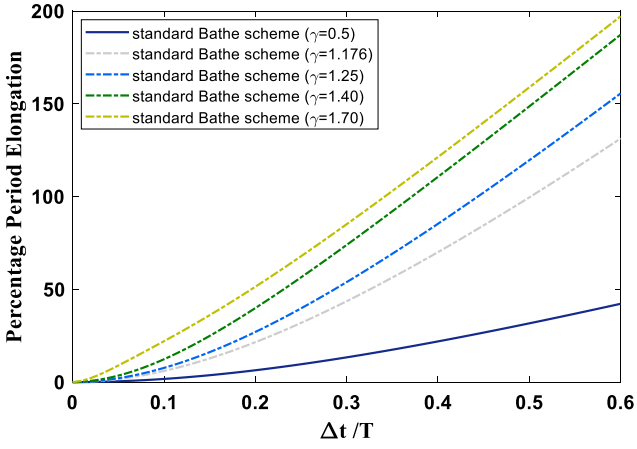

Fig. 3c. Percentage period elongation of standard Bathe scheme for various γ.

The standard Bathe method with $\gamma = 0.5$ has been widely employed for nonlinear analysis and is effective in many such applications, and in linear analysis. This scheme is equal to the β_1/β_2-Bathe method for $\beta_1 = 1/3$ and $\beta_2 = 2/3$, and is also equal to the ρ_∞-Bathe method when $\rho_\infty = 0$ and $\gamma = 0.5$. The advantage of its use is that no parameters need be set and only an appropriate size of time step needs to be selected – as it is always the case when using a direct integration method [1,10,11]. In structural dynamics solutions, the time step Δt is selected to accurately integrate all excited – and well represented – frequencies and mode shapes in the finite element model.

However in linear analysis it is of advantage to use the standard Bathe scheme method with $\gamma = 2 - \sqrt{2}$ because only one effective stiffness matrix is employed. In essence, the time integration scheme is used as, and performs like, a mode superposition solu-

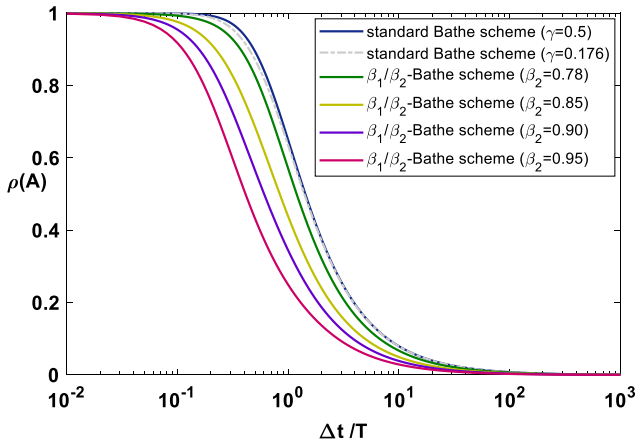

Fig. 4a. Spectral radius of the β_1/β_2- Bathe scheme with $\beta_1 = 0.43$ vs. standard Bathe scheme in *L*-stable state.

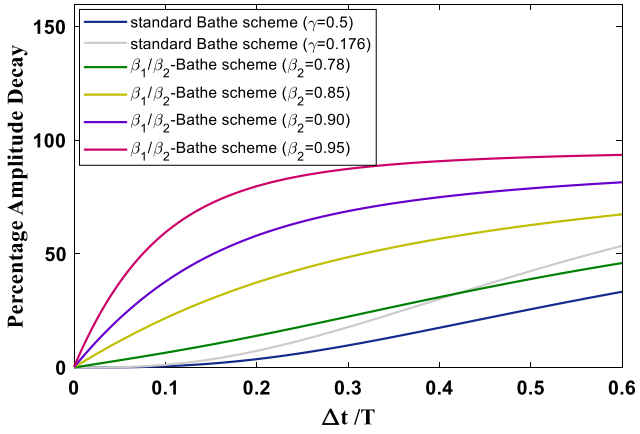

Fig. 4b. Percentage amplitude decay of the β_1/β_2- Bathe scheme with $\beta_1 = 0.43$ vs. standard Bathe scheme in *L*-stable state.

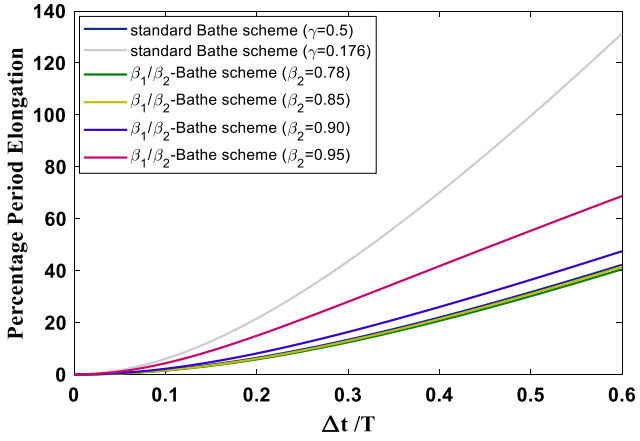

Fig. 4c. Percentage period elongation of the β_1/β_2- Bathe scheme with $\beta_1 = 0.43$ vs. standard Bathe scheme in *L*-stable state.

tion in linear analysis [1]. The use of only one effective stiffness matrix is also available for the β_1/β_2-Bathe method, see Section 3.6.

In some special cases, it may be of value to use the ρ_∞-Bathe method with a non-zero value for ρ_∞, that is $0 < \rho_\infty \leqslant 1.0$ because a large fraction of the finite element model frequencies is well representing the "exact" frequencies and is excited; we refer to Refs. [11,21,22] since we consider in the present paper only *L*-stable schemes of the Bathe methods. The Trapezoidal Rule corresponds to using $\rho_\infty = 1.0$.

In the solution of wave propagation problems, accurate solutions can be more difficult to obtain because many frequencies are excited and the CFL number, defined as CFL = $\Delta t/\Delta t_{cr}$ plays a crucial role, where Δt_{cr} is the critical time step for stability (typically of the Central Difference method [1]). The advantage of using an unconditionally stable scheme is of course that the CFL number is only used for accuracy considerations.

When using the standard Bathe method with $\gamma = 0.5$, or $\gamma = 2 - \sqrt{2}$, in the solution of wave propagation problems, it is frequently best to employ the time step given by CFL = 1 , see Refs. [12,24]. This use usually leads to acceptable answers. A smaller or larger CFL will not lead to an unstable solution but may give less accurate response predictions. Some solutions are given in Refs. [12,24] and below. The reason for a "good or optimal CFL" is that the dispersion errors due to the mesh (using traditional finite element discretizations) and the dispersion errors due to the time integration can cancel each other out to a high degree [26].

However, to reach more accuracy in the solutions, it can be of value to introduce more numerical damping and then the β_1/β_2-Bathe method may be effective because strong amplitude decay can be imposed while keeping the period elongation acceptable. This is, in particular, achieved using Eq. (26) and based on some limited numerical experimentation we found that reasonable values to use may be CFL = 1 with

$$\beta_1 = 0.43;\ \beta_2 = \left[2(1-\beta_1) - 0.5(16\beta_1^2 - 24\beta_1 + 8)^{0.5}\right] \approx 0.741$$

To then possibly achieve better accuracy we may try $0.741 \leqslant \beta_2 < 1$ where we recall that as we choose β_2 from 0.741 closer to 1, more numerical damping is applied.

However, we also found that the accuracy using the scheme to predict response is quite sensitive to the values used for the parameters. Only small changes can affect the solution accuracy of a specific problem, as we shall also see in the illustrative solutions presented next.

More experience with the values of parameters is needed in order to be able to give more focused recommendations.

6. Illustrative example solutions

In this section we present the solution of two example problems of wave propagations to illustrate our theoretical findings given above. We only use the Bathe schemes in these solutions, comparisons with other methods have been published in our earlier papers, see e.g. [11,22–24].

6.1. Wave propagations in a bi-material rod

We consider a bi-material rod created of two pieces with different material properties, see Fig. 5 [30]. The Young's moduli of the two pieces are $E_1 = 8 \times 10^3$ Pa and $E_2 = 8 \times 10^2$ Pa. The same Poisson's ratio = 0.0 and density = 1 kg/m^3 are assumed for each piece.

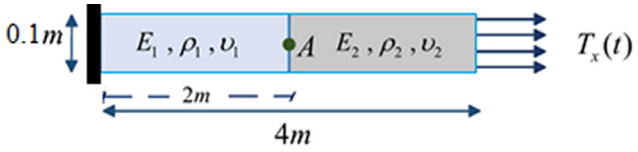

Fig. 5. A bi-material rod subjected to a unit step traction [30].

Hence the wave speeds are $c_1 = \sqrt{E_1/\rho_1} = 40\sqrt{5}$ and $c_2 = \sqrt{E_2/\rho_2} = 20\sqrt{2}$, respectively.

The rod is fixed at its left end, and a uniform constant step traction of unit value is applied at its right end. The resulting wave is reflected and refracted at the boundary of the materials.

We use a mesh of 800 traditional linearly interpolated elements to represent the rod, with each piece modeled by 400 equal-size elements, and use the time steps

$$\Delta t_1 = \text{CFL} \times \frac{\Delta x}{c_1} = \text{CFL} \times \frac{0.005}{40\sqrt{5}}$$

$$\Delta t_2 = \text{CFL} \times \frac{\Delta x}{c_2} = \text{CFL} \times \frac{0.005}{20\sqrt{2}}$$

with CFL = 1 for either the softer or the stiffer material. Hence we use either $\Delta t_1 = 5.59 \times 10^{-5}$ or $\Delta t_2 = 1.767 \times 10^{-4}$ for the entire structure, which means that CFL $\neq 1$ for the entire structure in a solution obtained with the consistent mass matrix.

For solving this problem, we use the standard Bathe method for different values of γ (which is the L-stable state of the ρ_∞- Bathe scheme) and the β_1/β_2- Bathe method. The solutions obtained using these methods are compared with one another and with the reference solution given in ref. [30].

The solutions for $\Delta t = \Delta t_1$ are shown in Figs. 6a–6f. For this time step the solution using the standard Bathe method with $\gamma = 0.5$ shows significant spurious oscillations. To suppress these oscillations, we have to apply numerical damping with a smaller fall-value for $\rho_\infty(\mathbf{A})$. Using the method, we first use $\gamma = 1.7$(Fig. 6b). Then we increase the value of γ to decrease the fall-value even further (Fig. 6c). Using the β_1/β_2- Bathe method, we employ $\beta_1 = 0.43$ and $\beta_2 = 0.741, 0.83, 0.86$ (Figs. 6d–6f). For this time step, the performance of the two methods to suppress the spurious oscillations is acceptable, but the β_1/β_2- Bathe scheme performs here slightly better.

When using $\Delta t = \Delta t_2$ the spurious oscillations in the solution using the standard Bathe method with $\gamma = 0.5$ are much less than when using $\Delta t = \Delta t_1$ (Fig. 7a). To suppress these small spurious oscillations, we used the parameters given in Figs. 7a–7f and we see that the β_1/β_2- Bathe method worked well giving a better prediction for the parameters used.

Of course, we only employed a certain set of parameter values for the standard and β_1/β_2-Bathe methods to illustrate how their choice affects the solutions and acceptable results may be obtained. Different values of parameters will yield different response predictions, but an important observation is that while the numerical damping can help to suppress spurious oscillations, it may also lead to a loss of accuracy.

6.2. Analysis of a prestressed square membrane

We consider a square prestressed membrane subjected to a constant initial velocity prescribed over its central domain, the

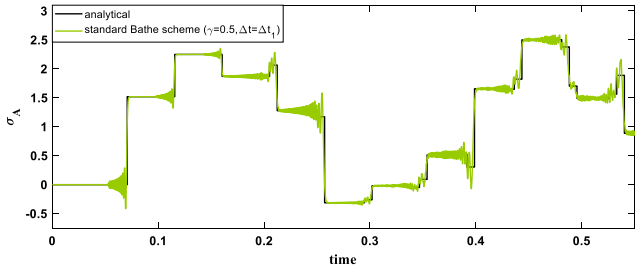

Fig. 6a. Predicted horizontal stress at point A using standard Bathe scheme.

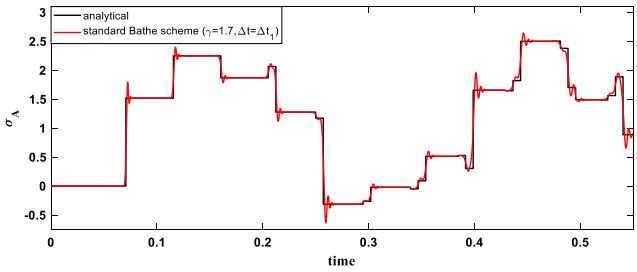

Fig. 6b. Predicted horizontal stress at point A using standard Bathe scheme.

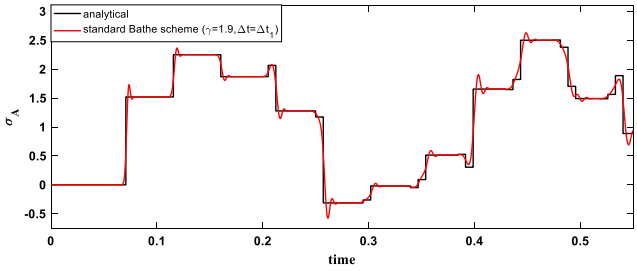

Fig. 6c. Predicted horizontal stress at point A using standard Bathe scheme.

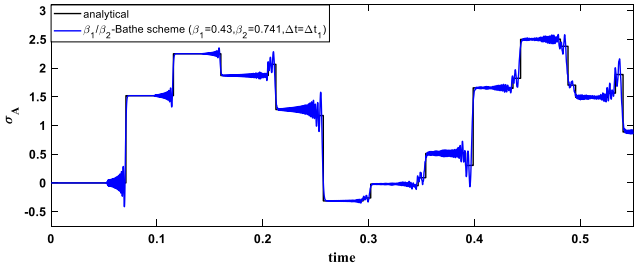

Fig. 6d. Predicted horizontal stress at point A using β_1/β_2- Bathe scheme.

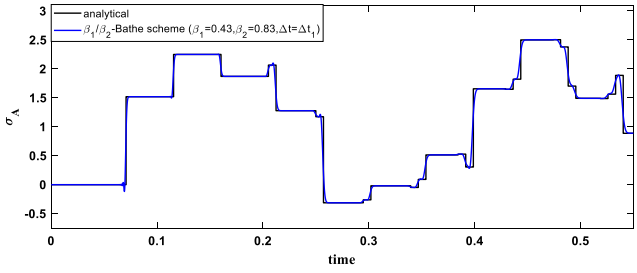

Fig. 6e. Predicted horizontal stress at point A using β_1/β_2- Bathe scheme.

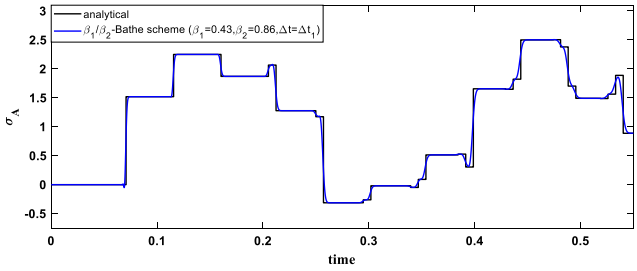

Fig. 6f. Predicted horizontal stress at point A using β_1/β_2- Bathe scheme.

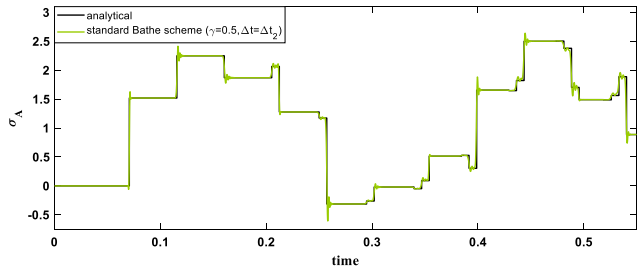

Fig. 7a. Predicted stress at point A using the standard Bathe scheme.

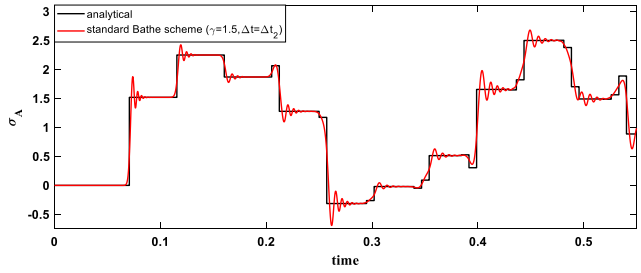

Fig. 7b. Predicted stress at point A using the standard Bathe scheme.

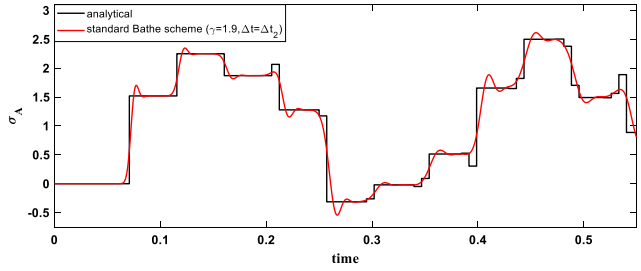

Fig. 7c. Predicted stress at point A using the standard Bathe scheme.

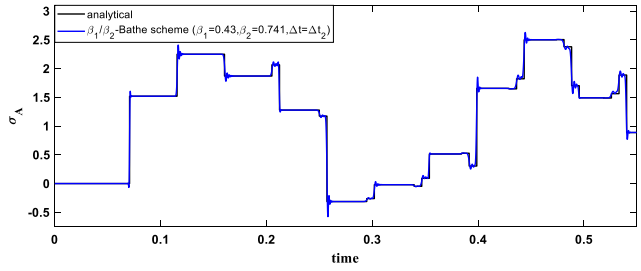

Fig. 7d. Predicted stress at point A using the β_1/β_2- Bathe scheme.

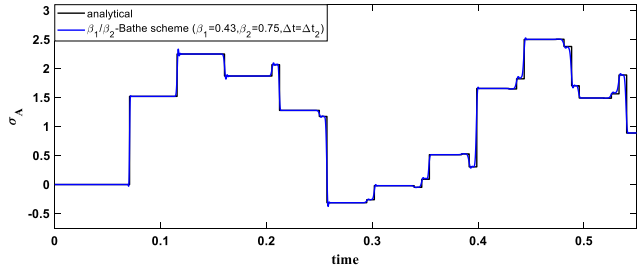

Fig. 7e. Predicted stress at point A using the β_1/β_2- Bathe scheme.

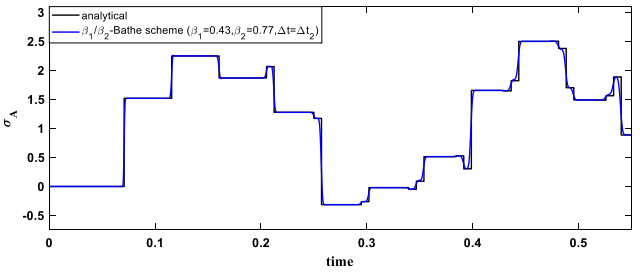

Fig. 7f. Predicted stress at point A using the β_1/β_2- Bathe scheme.

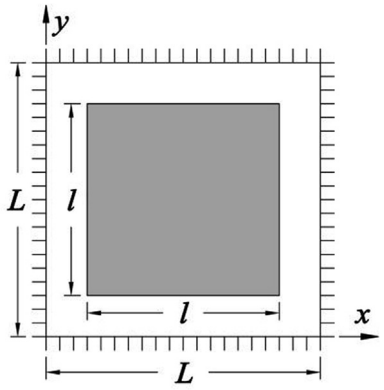

Fig. 8. A square membrane, L = 10 m and l = 7 m.

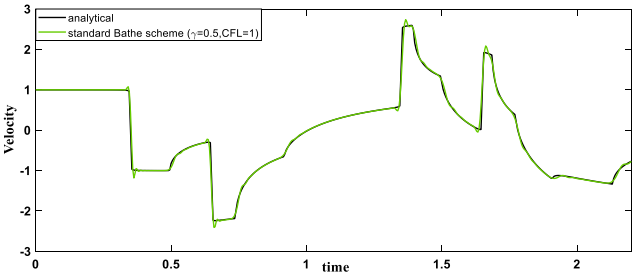

Fig. 9a. Predicted velocity at center point using standard Bathe scheme, $\gamma = 0.5$ and CFL = 1.

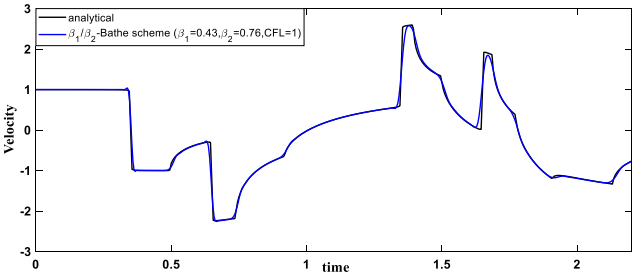

Fig. 9b. Predicted velocity at center point using β_1/β_2- Bathe scheme, CFL = 1.

gray area in Fig. 8 [15,31]. The wave velocity and mass density of the membrane are $c = 10\ m/s$ and $\rho = 1\ \mathrm{kg/m^3}$, respectively. Due to symmetry, we only discretize a quarter of the membrane and use a mesh of $120 \times 120 = 14{,}400$ 4-node square elements with the consistent mass matrix.

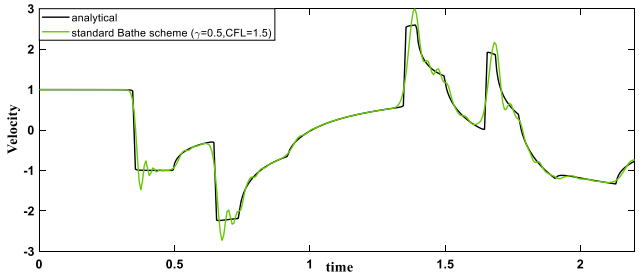

Fig. 10a. Predicted velocity at center point using standard Bathe scheme, $\gamma = 0.5$ and CFL = 1.5.

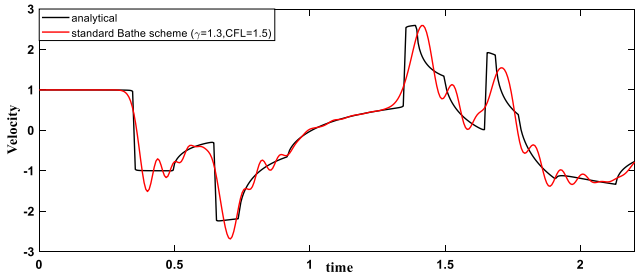

Fig.10b. Predicted velocity at center point using standard Bathe scheme, $\gamma = 1.3$ and CFL = 1.5.

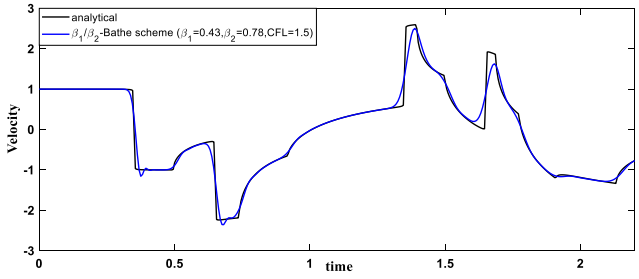

Fig. 10c. Predicted velocity at center point using β_1/β_2- Bathe scheme, CFL = 1.5.

The size of time step is given by

$$\Delta t = \text{CFL} \times \frac{\Delta x}{c} = \frac{\text{CFL}}{240}$$

In this problem solution the material conditions are uniform and hence we expect reasonable results using the standard Bathe method with $\gamma = 0.5$, CFL = 1. This is indeed the case. Figs. 9a-9c show that reasonable results compared to the reference solution [31] are obtained and also show a good response solution using the β_1/β_2- Bathe scheme. However, when using CFL = 1.5, because the use of a larger time step is of interest, the standard Bathe method with $\gamma = 0.5$ does not give accurate results, and the use of $\gamma = 1.3$ does not improve the accuracy of the response prediction, see Figs. 10a-10b. On the other hand, when using the β_1/β_2-Bathe scheme with the selected values of parameters the results are better and quite reasonable, see Fig.10c.

7. Concluding remarks

Our objective in this paper was to further investigate the β_1/β_2-Bathe method and provide some new insights. We focused on the stability and accuracy of the β_1/β_2-Bathe method in the *L*-stable state. The time step splitting ratio γ was calculated as a function of β_1 and β_2 to ensure *L*-stability for $0 < \gamma < 1$. The scheme is then a two-parameter method and if the parameter β_2 is selected judiciously as a function of β_1 we have a one-parameter scheme. We showed the spectral radii, amplitude decays and period elongations for various values of the parameters β_1 and β_2.

The key point is that for an accurate solution of transient problems using traditional spatial finite element discretizations, it is frequently necessary to introduce numerical damping. The damping has to be imposed by the time integration scheme such as to eliminate spurious oscillations while at the same time not deteriorating the overall accuracy of the response prediction. The standard Bathe scheme and the ρ_∞- Bathe method are frequently effective but improvements are clearly desirable and for this reason we further investigated the β_1/β_2-Bathe scheme.

Through a comparison of the β_1/β_2-Bathe and the standard Bathe scheme (which is the ρ_∞- Bathe method when $\rho_\infty = 0.0$, that is, *L*-stable) we showed that the period elongation error of the β_1/β_2-Bathe method is significantly less than provided by the standard Bathe method (using γ as a parameter) when amplitude decay is sought, that is, when we use value of the parameters that lead to a smaller "fall-value" of the spectral radius. We illustrated the use of the integration techniques in some example solutions but did not find "universally" effective values for β_1 and β_2.

The major disadvantage in the use of the β_1/β_2-Bathe method is that good values for the parameters need to be identified by numerical experimentation. The advantage using the standard Bathe scheme with $\gamma = 0.5$ and CFL = 1 is that no parameter is chosen or adjusted. Of course, if the β_1/β_2-Bathe, the standard Bathe scheme or ρ_∞-Bathe method are used with numerical experimentation, more accurate results may be reached, and then the β_1/β_2-Bathe method may give the best accuracy, but the actual improvement in accuracy depends on the problem solved.

Although no "breakthrough" for a drastically better performance than when using the standard Bathe scheme was discovered, we believe that the given study gives important insight and places the Bathe time integration schemes on a stronger foundation.

The experience gained through this work shows also once more the difficulties encountered when using "traditional spatial finite element discretizations" to solve wave propagation problems. A smaller time step does not necessarily lead to a smaller solution error. On the other hand, using the "overlapping finite elements" provides a much more powerful approach since the spatial dispersion errors can be uniformly reduced by refining the mesh and the temporal errors are reduced by decreasing the time step size, see Refs. [25–26] and the references given therein.

Declaration of Competing Interest

The authors declare that they have no known competing financial interests or personal relationships that could have appeared to influence the work reported in this paper.

References

[1] Bathe KJ. Finite Element Procedures. Prentice Hall, 1996; 2nd ed. KJ Bathe, Watertown, MA, 2014; also published by Higher Education Press China; 2016.
[2] Houbolt JC. A recurrence matrix solution for the dynamic response of aircraft. J Aeronaut Sci 1950;17:540–50.
[3] Newmark NM. A method of computation for structural dynamics. J Eng Mec Div, ASCE 1959;85(3):67–94.
[4] Wilson EL, Farhoomand I, Bathe KJ. Nonlinear dynamic analysis of complex structures. Int J Earthquake Eng Struct Dyn 1972;1(3):241–52.
[5] Bathe KJ, Wilson EL. Stability and accuracy analysis of direct integration methods. Int J Earthquake Eng Struct Dyn 1972;1(3):283–91.
[6] Benitez JM, Montans FJ. The value of numerical amplification matrices in time integration methods. Comput Struct 2013;128:243–50.
[7] Hilber HM, Hughes TJR, Taylor RL. Improved numerical dissipation for time integration algorithms in structural mechanics. Earthquake Eng Struct Dyn 1977;5(3):283–92.

[8] Chung J, Hulbert GM. A time integration algorithm for structural dynamics with improved numerical dissipation: the Generalized-alpha method. J Appl Mech Trans ASME 1993;60:371–5.
[9] Bathe KJ, Baig MMI. On a composite implicit time integration procedure for nonlinear dynamics. Comput Struct 2005;83:2513–24.
[10] Bathe KJ. Conserving energy and momentum in nonlinear dynamics: a simple implicit time integration scheme. Comput Struct 2007;85:437–45.
[11] Bathe KJ, Noh G. Insight into an implicit time integration scheme for structural dynamics. Comput Struct 2012;98:1–6.
[12] Noh G, Ham S, Bathe KJ. Performance of an implicit time integration scheme in the analysis of wave propagations. Comput Struct 2013;123:93–105.
[13] Noh G, Bathe KJ. An explicit time integration scheme for the analysis of wave propagations. Comput Struct 2013;129:178–93.
[14] Shojaee S, Rostami S, Abbasi A. An unconditionally stable implicit time integration algorithm: modified quartic B-spline method. Comput Struct 2015;153:98–111.
[15] Soares D. A novel family of explicit time marching techniques for structural dynamics and wave propagation models. Comput Methods Appl Mech Eng 2016;311:838–55.
[16] Kwon SB, Lee JM. A non-oscillatory time integration method for numerical simulation of stress wave propagations. Comput Struct 2017;192:248–68.
[17] Noh G, Bathe KJ. Further insights into an implicit time integration scheme for structural dynamics. Comput Struct 2018;202:15–24.
[18] Kim W, Lee JH. An improved explicit time integration method for linear and nonlinear structural dynamics. Comput Struct 2018;206:42–53.
[19] Malakiyeh MM, Shojaee S, Hamzehei-Javaran S. Development of a direct time integration method based on Bezier curve and 5th-order Bernstein basis function. Comput Struct 2018;194:15–31.
[20] Malakiyeh MM, Shojaee S, Hamzehei-Javaran S, Tadayon B. Further insights into time-integration method based on Bernstein polynomials and Bezier curve for structural dynamics. Int J Struct Stab Dyn 2019;1950113.
[21] Malakiyeh MM, Shojaee S, Bathe KJ. The Bathe time integration method revisited for prescribing desired numerical dissipation. Comput Struct 2019;212:289–98.
[22] Noh G, Bathe KJ. The Bathe time integration method with controllable spectral radius: the ρ_∞- Bathe method. Comput Struct 2019;212:299–310.
[23] Noh G, Bathe KJ. For direct time integrations: a comparison of the Newmark and ρ_∞- Bathe method schemes. Comput Struct 2019;225:1–12.
[24] Kwon SB, Bathe KJ, Noh G. An analysis of implicit time integration schemes for wave propagations. Comput Struct 2020;230:106188.
[25] Bathe KJ. The AMORE paradigm for finite element analysis. Adv Eng Softw 2019;130:1–13.
[26] Chai Y, Bathe KJ. Transient wave propagation in inhomogeneous media with enriched overlapping triangular elements. Comput Struct 2020;237:106273.
[27] Bathe KJ. Frontiers in finite element procedures & applications. Chapter 1 in computational methods for engineering technology. In: Topping BHV, Iványi P, editors. Saxe-Coburg Publications, Stirlingshire, Scotland; 2014.
[28] Kroyer R, Nilsson K, Bathe KJ. Advances in direct time integration schemes for dynamic analysis. Automotive CAE Companion 2016;2017:32–5.
[29] Nilsson K, Tornberg F. On blowdown analysis with efficient and reliable direct time integration methods for wave propagation and fluid-structure-interaction response. Comput Struct 2019;216:1–14.
[30] Izadpanah E, Shojaee S, Hamzehei-Javaran S. A time-dependent discontinuous Galerkin finite element approach in two-dimensional elastodynamic problems based on spherical Hankel element framework. Acta Mech 2018;229:4977–94.
[31] Mansur WJ. A time-stepping technique to solve wave propagation problems using the boundary element method Ph.D. Thesis. England: University of Southampton; 1983.